

Suppression of dense Kondo state in CeB₆ under pressure

N. Foroozani,¹ J. Lim,¹ G. Fabbris,^{1,2} P. F. S. Rosa,³ Z. Fisk,³ and J. S. Schilling^{1,*}

¹*Department of Physics, Washington University, St. Louis, MO 63130, USA*

²*Advanced Photon Source, Argonne National Laboratory, Argonne, IL 60439, USA*

³*Department of Physics and Astronomy, University of California, Irvine, CA 92697, USA*

(Dated: February 29, 2024)

To investigate whether the dense Kondo compound CeB₆ might evolve into a topological insulator under sufficient pressure, four-point electrical resistivity measurements have been carried out over the temperature range 1.3 K to 295 K in a diamond anvil cell to 122 GPa. The temperature T_{max} of the resistivity maximum initially increases slowly with pressure but disappears between 12 and 20 GPa. The marked changes observed under pressure suggest that a valence and/or structural transition may have occurred. Synchrotron x-ray diffraction measurements, however, fail to detect any change in crystal structure to 85 GPa. Although a transition into an insulating phase is not observed, this dense Kondo system is completely suppressed at 43 GPa, leaving behind what appears to be a conventional Fermi liquid metal.

I. INTRODUCTION

Many compounds and alloys containing Ce, including Ce metal, show highly anomalous magnetic properties due to the fact that the $4f$ level in trivalent Ce often lies near a magnetic instability. This led to the observation of a classic Kondo effect in the electrical resistivity measurements of Winzer¹ on the dilute magnetic alloy (La_{0.994}Ce_{0.006})B₆ to 50 mK; in these studies the Kondo temperature is estimated to lie near $T_K \approx 1$ K. At higher Ce concentrations the competition between the Kondo effect and Ce-Ce exchange interactions increases, leading finally in CeB₆ to an exotic phase diagram with a prominent resistivity maximum near 4 K and two kinds of ordered phases: antiferroquadrupolar ordering below 3.2 K (phase II) and antiferromagnetic ordering below 2.3 K (phase III)^{2,3}. This compound has attracted a great deal of attention following its identification as a dense Kondo system⁴. CeB₆ is metallic at ambient pressure with the simple cubic ($Pm\bar{3}m$) structure⁵. The ground state of the Ce³⁺ ion is a Γ_8 quartet split by 30 K into two doublets and separated by 540 K from the excited Γ_7 doublet⁶.

SmB₆ is a prime candidate for a topological Kondo insulator categorized as a heavy fermion semiconductor^{7–10} with strong electron-electron correlations in which the localized $4f$ electrons give rise to novel ground states^{11,12}. SmB₆ and CeB₆ both have the $J = 5/2$ Hund's rule configuration^{6,13}. Upon cooling below 10 K, the electrical resistivity of SmB₆ rises by orders of magnitude as it enters into an anomalous insulating state, only to saturate near $7 \text{ m}\Omega\text{cm}$ ¹⁴. This behavior agrees with that of a Kondo insulator where at high temperatures highly correlated electron behavior is observed, but at the lowest temperatures an insulating state emerges as a bulk band gap opens up through the hybridization of localized $4f$ states with $5d$ conduction electrons^{7–10}. Since the primary effect of high pressure on a dense Kondo system is to enhance this hybridization¹⁵, it is conceivable that sufficient pressure might succeed in transporting CeB₆ into the topological Kondo insulator regime.

To date there have been relatively few studies of the transport and magnetic properties of CeB₆ at high pressures^{15–17}. Kobayashi *et al.*¹⁵ report that the prominent resistivity maximum in CeB₆ shifts from 3.6 K to ~ 7 K at 13 GPa pressure, but there is no evidence for a transition to a Kondo insulating state as in SmB₆¹⁴. There is also no evidence for a structural phase transition in CeB₆ at ambient temperature to 20 GPa¹⁸.

In the present study we extend the previous resistivity experiments to significantly higher pressures (122 GPa). The resistivity maximum is found to initially shift to somewhat higher temperatures with pressure, but rapidly decrease in magnitude, finally disappearing completely at 20 GPa. The present experiments fail to find any evidence that CeB₆ transforms into a Kondo insulating state to 122 GPa in the temperature range 1.3 - 295 K. However, pressures of 43 GPa and above are sufficient to completely suppress the anomalies associated with CeB₆'s dense Kondo state. These dramatic changes under pressure are not due to structural phase transitions, as evidenced by x-ray diffraction studies at 15 K to 85 GPa. However, we cannot exclude the possibility that a pressure-induced change in Ce's valence (Ce⁺³ to Ce⁺⁴) may have occurred.

II. EXPERIMENTAL METHODS

Single crystals of CeB₆ were grown in Al flux by slow cooling from 1450°C. The crystals were removed from the Al flux by leaching in NaOH solution¹⁹. The lattice parameter of the resulting simple cubic crystals was measured to be $4.132(4) \text{ \AA}$.

High pressure dc electrical resistivity measurements were carried out in a diamond-anvil cell (DAC) using two opposing 1/6-carat, type-Ia diamond anvils with 0.35 mm culets beveled at 7° to 0.18 mm central flats. A Re gasket (6-7 mm diameter, 250 μm thick) was preindented to 30 μm and insulated using a 4:1 c-BN-epoxy mixture which also served as a quasi-hydrostatic pressure medium. The pressure was determined *in situ* by placing two small

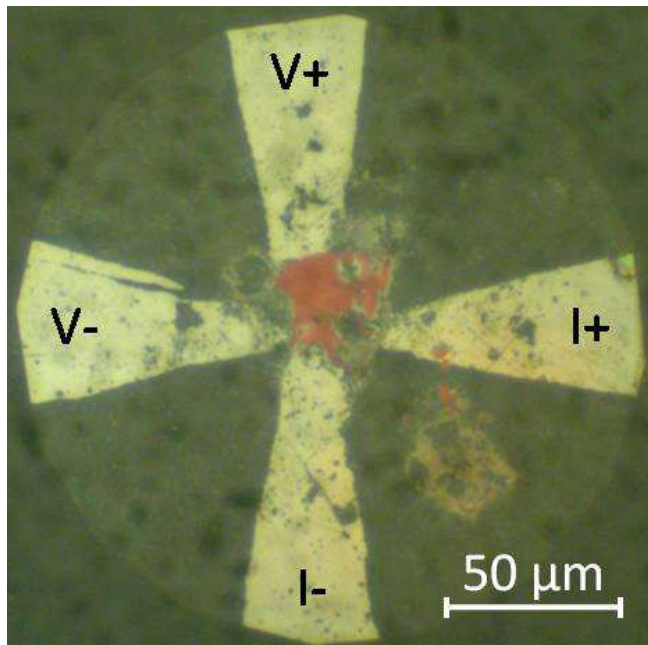


FIG. 1. (color online) Image of red CeB_6 sample ($40 \times 40 \times 5 \mu\text{m}^3$) resting on four Pt leads ($4 \mu\text{m}$ thick) on insulated Re gasket.

ruby spheres²⁰ in the sample space. Four-point resistivity was measured using four leads cut from a thin Pt foil (see Fig. 1); two extra leads were connected to the Re gasket to detect any electrical shorts. A single crystal sample (dimensions $40 \times 40 \times 5 \mu\text{m}^3$) was placed on top of the Pt leads and electrical contact was made by pressing the sample into the leads with the opposing anvil. During the course of the experiment the sample was plastically deformed by the quasi-hydrostatic pressure. To keep the power dissipated in the sample below $1 \mu\text{W}$, an excitation current of $\sim 1 \text{ mA}$ was used. A reduction of the current to 0.1 mA at the lowest temperature (1.3 K) caused no measurable change in the sample resistance.

A He-gas driven membrane allowed changes in pressure at any temperature above 3 K . The pressure cell was placed in a continuous-flow cryostat (Oxford Instruments) and submerged in pumped liquid He to reach temperatures as low as 1.3 K . The pressure was determined either at ambient temperature (295 K) or at low temperature ($5\text{--}10 \text{ K}$) with a resolution of $\pm 0.2 \text{ GPa}$ using the revised ruby pressure scale of Chijioke *et al.*²¹. Raman spectroscopy²² on the diamond vibron was also used to determine the pressure in the upper pressure range where the ruby fluorescence became very weak. Further details of the high pressure resistivity techniques are given elsewhere²³.

High-pressure low-temperature powder x-ray diffraction (XRD) experiments were carried out at the HP-CAT (16-BM-D) beamline of the Advanced Photon Source, Argonne National Laboratory. A symmetric DAC (Princeton shops) was prepared using standard dia-

mond anvils with $300 \mu\text{m}$ diameter culets beveled to $180 \mu\text{m}$. The anvils were glued onto WC and B_4C seats, the latter allowing the extension of the 2θ range to $\sim 25^\circ$. A Re gasket was pre-indented to $25 \mu\text{m}$ and a hole $90 \mu\text{m}$ in diameter laser drilled through the center of the indentation to serve as sample chamber.

Powdered CeB_6 was placed into the sample chamber together with Au powder as pressure marker and a ruby sphere. He gas was then loaded using the GSE-CARS/COMPRES system²⁴ to $\sim 8.6 \text{ GPa}$ as determined by ruby fluorescence²¹. During the high-pressure x-ray experiment the *in situ* pressure was determined from the known equation of state of Au²⁵.

The pressure cell was cooled using a He flow cryostat. Isothermal measurements were performed at $\sim 15 \text{ K}$ and the pressure was increased at low temperature using a gear box. Photons of 29.2 keV energy compressed the reciprocal space, thus allowing a significant number of Bragg reflections within the limited 2θ range. Diffraction was detected in angular dispersive mode using an image plate (MAR3450) with $100 \times 100 \mu\text{m}^2$ pixel size located 324.37 mm from the sample. The beam was focused to $\sim 15 \times 5 \mu\text{m}^2$ by a pair of Kirkpatrick-Baez mirrors. The 2D diffraction patterns were converted to intensity versus 2θ using Fit2D software²⁶. CeB_6 and Au diffraction patterns were concomitantly fit using Le Bail and Rietveld methods implemented with GSAS/EXPGUI software^{27,28}.

III. RESULTS OF EXPERIMENT

A. Electrical resistivity measurements

In Fig. 2 is shown resistance versus temperature for the high-pressure data obtained on CeB_6 over the temperature range 1.3 K to 295 K . The order of measurement is: $0.5, 7.7, 12, 20, 30, 43, 122 \text{ GPa}$. Above 10 K all data shown were taken with increasing temperature due to the relatively slow rate of warming to 295 K (12 hours). Pressure was always applied at 295 K . All values of pressure given in Fig. 2 were measured at 295 K before cooling down; the values of the pressure after cooling to $5\text{--}10 \text{ K}$ and after warming back up to 295 K , all at the same gas pressure in the membrane, are given in parentheses in the caption to Fig. 2, if they were measured. The highest pressure reached, 122 GPa , was determined from Raman scattering off the diamond vibron.

At 0.5 GPa the temperature-dependent resistance $R(T)$ displays a resistivity minimum near 110 K followed at lower temperatures by a peak near $T_{\text{max}} \approx 6 \text{ K}$, a somewhat higher temperature than $T_{\text{max}} \approx 3.5 \text{ K}$ reported in earlier measurements on CeB_6 in the $0\text{--}1 \text{ GPa}$ pressure range^{29–31}. Kobayashi *et al.*³¹ find that T_{max} shifts to higher temperatures with pressure, reaching 7 K at 13 GPa . From the data in Fig. 2 one also sees that T_{max} increases with pressure, the resistivity peak itself diminishing rapidly in size and finally disappearing be-

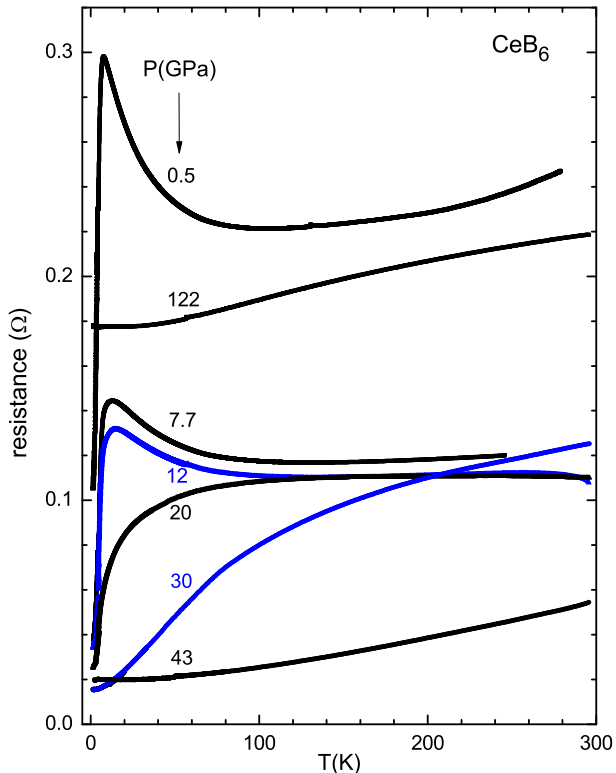


FIG. 2. (color online) Electrical resistance of CeB_6 versus temperature at pressures in GPa measured at 295 K before cooling. Numbers in parentheses after each pressure give pressures measured at 5-10 K after cooling (left) and at 295 K after warming back to 295 K (right): 0.5(1.2,0.8), 7.7(-,8.5), 12(-,14), 20(24.5,-), 30(35,31), 43(52,45), 122(-,129). A dash “-” indicates the pressure was not measured.

tween 12 and 20 GPa. For pressures up to and including 30 GPa, the resistance below 100 K decreases with pressure; for temperatures above 20 K the decrease in resistance between 30 and 43 GPa is particularly large. This decrease likely reflects the intrinsic pressure dependence of the CeB_6 sample since any plastic deformation of the sample by the solid pressure medium would be expected to *enhance* its resistance.

As the pressure was increased above 43 GPa, however, the resistance at ambient temperature began to shift upwards and change with time at a given pressure, indicating relaxation behavior in the pressure cell. The two ruby spheres were also seen to move away from the sample, preventing a reliable determination of the sample pressure. At 122 GPa the pressure was determined from the diamond anvil vibron using Raman spectroscopy. In Fig. 2 it is seen that the entire resistance curve $R(T)$ at 122 GPa has risen to a significantly higher value, *nine times* that at 43 GPa. The reason for the large increase in resistance is not clear, but could be the result of a structural phase transition with a mixed phase region,

leading to enhanced defect scattering. Alternatively, the outward flow of the pressure cell could generate a large number of lattice defects in the sample from plastic deformation by the solid pressure medium. In any case, to 122 GPa no sharp upturn in the electrical resistivity of CeB_6 below 10 K was observed that might have signaled a transition into a topological insulating state, as suggested for SmB_6 ¹⁴.

Following the measurement at 122 GPa, the pressure was released completely. The $R(T)$ dependence was similar to that at 122 GPa but shifted to even higher resistance values. In addition, the characteristic resistivity maximum seen near 6 K at 0.5 GPa was *not* recovered at ambient pressure. This finding would be consistent with a structural phase transition at extreme pressures that remained metastable after releasing to ambient pressure.

The dramatic changes observed in the temperature-dependent resistivity of CeB_6 under pressure from 0.5 to 43 GPa suggest that a change in valence and/or a structural transition may have taken place. Previous diffraction studies by Leger *et al.*¹⁸ at ambient temperature revealed no phase transition to 20 GPa. High pressure x-ray diffraction and x-ray absorption near-edge structure (XANES) studies to pressures of at least 50 GPa would be helpful to clarify the situation. We next discuss the results of our recent x-ray diffraction measurements on CeB_6 to pressures exceeding 50 GPa.

B. X-ray diffraction measurements

The x-ray diffraction pattern of CeB_6 at 15 K for selected hydrostatic pressures with He pressure medium is shown in Fig. 3. Neither the emergence of new Bragg peaks, nor the splitting of existing peaks, was observed to the highest pressure (85 GPa), indicating that the structure of CeB_6 remains simple cubic throughout this range.

The pressure dependence of the unit cell volume is well described by a 3rd order Birch-Murnaghan equation of state (see Fig. 4):

$$P(V) = \frac{3B_o}{2} \left[\left(\frac{V_o}{V} \right)^{7/3} - \left(\frac{V_o}{V} \right)^{5/3} \right] \times \left\{ 1 + \frac{3}{4} (B'_o - 4) \left[\left(\frac{V_o}{V} \right)^{2/3} - 1 \right] \right\}, \quad (1)$$

where P and V are the measured pressure and volume, respectively. The fit to the data using Eq. 1 yields the ambient pressure volume V_o , bulk modulus B_o , and pressure derivative of the bulk modulus B'_o . The fit parameters are summarized in Table I together with those reported in the literature. The first fit includes only the present $V(P)$ data measured from 8 to 85 GPa. The resulting black fit curve is seen in Fig. 4 to lie slightly below the ambient pressure volume V_o from Sirota *et al.*³². In Table I it can be seen that the value of V_o lies below the literature values, whereas the bulk modulus B_o lies above

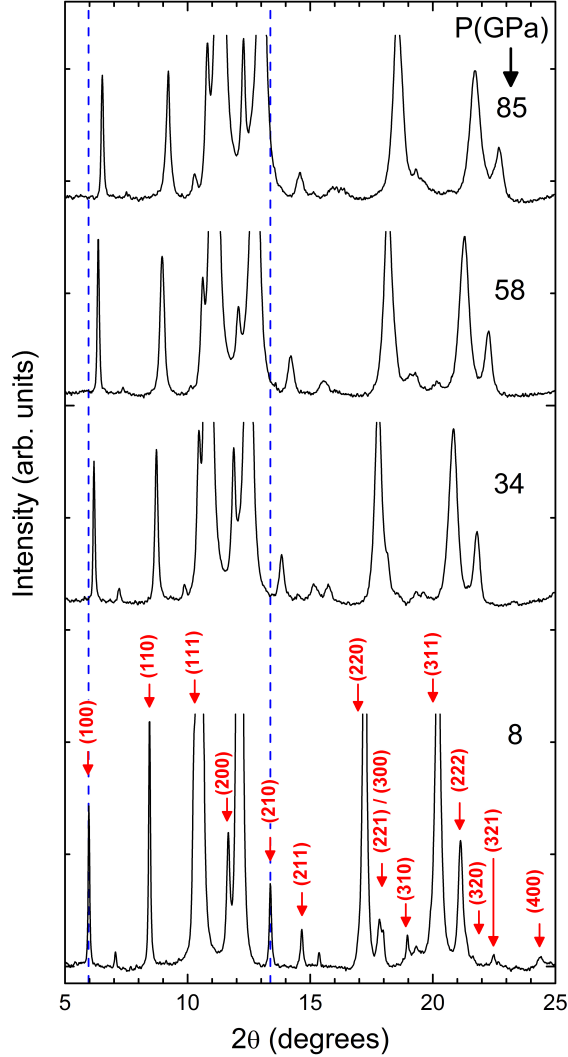


FIG. 3. (color online) CeB_6 diffraction pattern at 15 K and selected pressures. Large, truncated peaks are from Au marker. Red arrows and indices give positions of CeB_6 peaks; all other peaks can be assigned to Au, ruby or Re.

these values. Much better agreement is achieved if Eq. 1 is fit to the lowest 5 high pressure points to 20 GPa in Fig. 4, including the ambient pressure point from Sirota *et al.*³². This excellent agreement is not surprising since the literature studies were all carried out at pressures at or below 20 GPa.

Although no structural phase transition was detected to 85 GPa pressure, one cannot exclude the possibility of a change in structure in the region 85 - 122 GPa that led to the strong increase in $R(T)$ at 122 GPa.

IV. DISCUSSION

Pressures exceeding 43 GPa cause drastic changes in the temperature-dependent resistance $R(T)$ of CeB_6 that

indicate a complete suppression of its dense Kondo state. The prominent resistivity peak near ambient pressure disappears between 12 and 20 GPa and $R(T)$ is strongly suppressed over nearly the entire measured temperature range as the pressure is increased to 43 GPa.

It is well known that in Ce systems exhibiting Kondo effect phenomena, the Kondo temperature T_K increases rapidly with pressure³³. In the dilute magnetic alloy $(\text{La}_{0.994}\text{Ce}_{0.006})\text{B}_6$ the electrical resistivity decreases with increasing temperature from its giant unitarity limit value and passes through a minimum near $T_{\min} \approx 20$ K before rising rapidly as the phonons of the stiff LaB_6 host lattice become thermally excited; the Kondo temperature in this dilute magnetic alloy is estimated to lie near 1 K¹. The increase in T_K with pressure comes from the increasing hybridization between the 4f and conduction electrons that enhances the negative covalent mixing exchange interaction responsible for the Kondo phenomena. As T_K increases with pressure, the temperature of the resistivity minimum T_{\min} in a dilute Kondo system would be expected to first slowly increase with pressure, but then begin to decrease after T_K becomes larger than T_{\min} ³³.

In the dense Kondo compound CeB_6 , T_{\min} lies near 110 K at both ambient^{29,30} and 0.5 GPa pressure (see Fig. 2). The higher value of T_{\min} for CeB_6 (110 K) compared to that for the dilute magnetic alloy (20 K) is due to the much higher Ce concentration in the former. The marked resistivity maximum in CeB_6 arises from magnetic Ce-Ce interactions and coherence effects in the Kondo lattice. Due to the increase of its Kondo temperature with pressure, T_{\min} for CeB_6 increases with pressure from 0.5 GPa to 7.7 GPa to 12 GPa, disappearing com-

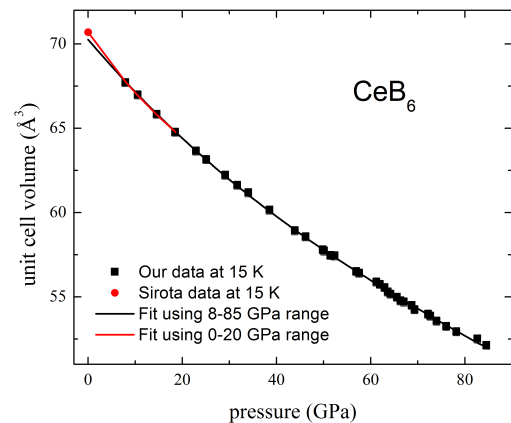


FIG. 4. (color online) Pressure dependence of unit cell volume of CeB_6 at 15 K. Error bars are smaller than symbols. Data are fit 3rd order Birch-Murnaghan equation of state. Black curve fits present data 8-85 GPa. Red curve fits 4 data points 8-20 GPa plus point at 0 GPa from Sirota *et al.* in Ref³². Fit parameters are given in Table I.

TABLE I. Summary of literature values of unit cell volume of CeB₆ at ambient pressure V_o , bulk modulus B_o , and pressure derivative of bulk modulus B'_o compared to present results (see Fig. 4).

Method	P (GPa)	Reference	T (K)	V_o (Å ³)	B_o (GPa)	B'_o
x-ray	8-85	this paper	15	70.3(3)	204(10)	2.5
x-ray	0-20	this paper	15	70.69(9)	167(8)	5.4
x-ray	0	32	15	70.7	-	-
x-ray	0-20	18	300	71.27	166	3.2
x-ray	0-10	16	300	70.86	159	-
ultrasound	0	35	10	-	191	-
ultrasound	0	36	300	-	168	-
Bril. scatt.	0	36	300	-	182	-
DFT	0	37	300	72.47	173	3.9
DFT	0	38	0	71.16	162	-

pletely at 20 GPa and above. However, it is difficult to understand why the resistivity of CeB₆ does not increase over the measured temperature range as the Kondo temperature moves to ever higher temperatures, as would be expected for a dilute magnetic Kondo alloy³³.

The unexpected overall rapid decrease in $R(T)$ for CeB₆ as the pressure increases to 43 GPa could be taken to suggest that a valence transition occurs in the Ce cation. A pressure-induced change of Ce's valence from Ce⁺³ to Ce⁺⁴ would leave the Ce cation devoid of 4*f* electrons and, therefore, completely quench the dense Kondo state, whereby $R(T)$ would decrease significantly. At 43 GPa the temperature dependence of the resistivity looks much like that of a conventional Fermi liquid metal. Unfortunately, the signal/noise ratio in this experiment is not sufficient to establish whether or not the relation $\rho(T) \propto T^2$ holds, as one would expect from a Fermi liquid at sufficiently low temperatures.

The valence-change scenario receives some support from the fact that the temperature-dependent part of the resistivity at 43 GPa can be estimated³⁴ to change by only $\Delta R \approx 9 \mu\Omega\text{cm}$ from 295 K to 1.3 K. This value of ΔR is well below than that found for pure La³⁹, which contains no 4*f* electrons, and is only about six times greater than that for pure copper, one of the best conductors known. It would be of considerable interest to carry out XANES measurements on CeB₆ to pressures of at least 50 GPa to establish whether or not Ce in CeB₆ undergoes a valence change from Ce⁺³ to Ce⁺⁴.

In summary, electrical resistivity measurements on CeB₆ from 1.3 K to 295 K to pressures as high as 122 GPa fail to find any evidence for a transition into a topological insulating state. However, pressures of 43 GPa are found to completely transform CeB₆ from a dense Kondo system into what appears to be an ordinary Fermi liquid metal. Future high-pressure synchrotron spectroscopy studies are recommended to shed light on the exact nature of this transformation and to establish whether or not it is driven by an increase in valence.

ACKNOWLEDGMENTS

The authors would like to express gratitude to T. Matsuoka and K. Shimizu for sharing information on their high-pressure electrical resistivity techniques used in this study. Thanks are due A. Gangopadhyay for his critical reading of the manuscript. This work was supported by the National Science Foundation (NSF) through Grant No. DMR-1104742 and by the Carnegie/DOE Alliance Center (CDAC) through NNSA/DOE Grant No. DE-FC52-08NA28554. Work at Argonne National Laboratory is supported by the U.S. Department of Energy, Office of Science, under contract No. DE-AC02-06CH11357.

* Corresponding author: jss@wuphys.wustl.edu

¹ K. Winzer, Solid State Commun. **16**, 521 (1975).

² K. Winzer and W. Felsh, J. Phys. (Paris) **39**, C6-832 (1978).

³ R. Shiina, H. Shiba, and P. Thalmeier, J. Phys. Soc. Japan **66**, 1741 (1997).

⁴ T. Kasuza, K. Takegahara, Z. Aoki, K. Hanyawa, M. Kasaza, S. Kunii, T. Fujita, N. Sato, H. Kimura, T. Komatsubara, T. Furuno, and J. Rossat-Mignod, in *Valence Fluctuations in Solids*, L. M. Falicov, W. Hanke, M. B. Maple, editors (North-Holland, Amsterdam, 1981) p. 215.

⁵ J. M. Leger, Revue Phys. Appl. **19**, 815 (1984).

⁶ E. Zirngiebl, B. Hillebrands, S. Blumenröder, G. Güntherodt, M. Löwenhaupt, J. M. Carpenter, K. Winzer, and Z. Fisk, Phys. Rev. B **30**, 4052 (1984).

⁷ G. Aeppli and Z. Fisk, Comm. Condens. Matter Phys. **16**, 155 (1992).

⁸ P. Riseborough, Adv. Phys. **49**, 257 (2000).

⁹ P. W. Anderson, Phys. Rev. Lett. **104**, 176403 (2010).

¹⁰ P. Coleman, in *Handbook of Magnetism and Advanced Magnetic Materials*, Vol 1 (Wiley, 2007) pps. 95-148.

¹¹ J. Jiang, S. Li, T. Zhang, Z. Sun, F. Chen, Z. R. Ye, M. Xu, Q. Q. Ge, S. Y. Tan, X. H. Niu, M. Xia, B. P. Xie, Y. F. Li, X. H. Chen, H. H. Wen, and D. L. Feng, Nat. Commun. **4**, 3010 (2013).

¹² M. Neupane, N. Alidoust, S.-Y. Xu, T. Kondo, Y. Ishida, D. J. Kim, C. Liu, I. Belopolski, Y. J. Jo, T.-R. Chang, H.-T. Jeng, T. Durakiewicz, L. Balicas, H. Lin, A. Bansil, S. Shin, Z. Fisk, and M. Z. Hasan, Nat. Commun. **4**, 2991 (2013).

¹³ P. Nyhus, S. L. Cooper, Z. Fisk, and J. Sarrao, Phys. Rev. B **55**, 12488 (1997); P. A. Alekseev, V. N. Lazukov, R. Osborn, B. D. Rainford, I. P. Sadikov, E. S. Konovalova, and Yu. B. Paderno, Europhys. Lett. **23**, 347 (1993).

- ¹⁴ M. Neupane et al., Nature Commun. (2013).
- ¹⁵ T. C. Kobayashi, K. Hashimoto, S. Eda, K. Shimizu, K. Amaya, and Y. Onuki, Physica B **281-282**, 553 (2000).
- ¹⁶ N. B. Brandt, V. V. Moshchalkov, S. N. Pashkevich, M. G. Vybornov, and M. V. Semenov, Solid State Comm. **56**, 937-941 (1985).
- ¹⁷ M. Takashita, H. Aoki, C. J. Haworth, T. Terashima, S. Uji, C. Terakura, T. Matsuomoto, A. Uesawa, T. Suzuki, R. Settai, Y. Onuki, N. Sato, S. Kunii, T. Nishigaki, H. Sugawara, Y. Aoki, H. Sato, Rev. High Pressure Sci. Technol. **7**, 456 (1998).
- ¹⁸ J. M. Leger, J. Rossat-Mignod, S. Kunii, and T. Kasuya, Solid State Comm. **54**, 995-997 (1985).
- ¹⁹ P. C. Canfield and Z. Fisk, Phil. Mag. B **65**, 1117 (1992).
- ²⁰ J. C. Chervin, B. Canny, and M. Mancinelli, High Pressure Res. **21**, 305 (2001)
- ²¹ A. D. Chijioke, W. J. Nellis, A. Soldatov, and I. F. Silvera, J. Appl. Phys. **98**, 114905 (2005).
- ²² Y. Akahama and H. Kawamura, J. Appl. Phys. **100**, 043516 (2006).
- ²³ K. Shimizu, K. Amaya, and N. Suzuki, J. Phys. Soc. Jpn. **74**, 1345 (2005).
- ²⁴ M. Rivers, V. B. Prakapenka, A. Kubo, C. Pullins, C. M. Holl, and S. D. Jacobsen, High Press. Res. **28**, 273-292 (2008).
- ²⁵ W. B. Holzapfel, M. Hartwig, and W. Sievers, J. Phys. Chem. Ref. Data **30**, 515-529 (2001).
- ²⁶ A. P. Hammersley, S. O. Svensson, M. Hanfland, A. N. Fitch, and D. Häusermann, High Press. Res. **14**, 235 (1996).
- ²⁷ A. C. Larson and R. B. Von Dreele, Los Alamos National Laboratory Report LAUR, 86-748 (1994).
- ²⁸ B. H. Toby, J. Appl. Cryst. **34**, 210-213 (2001).
- ²⁹ N. E. Sluchanko, A. V. Bogach, V. V. Glushkov, S. V. Demishev, V.Yu. Ivanov, M. I. Ignatov, A. V. Kuznetsov, N. A. Samarin, A. V. Semeno, and N.Yu. Shitsevalova, J. Exper.Theor. Phys. **104**, 120 (2007).
- ³⁰ N. Môri, N. Sato, and T. Kasuya, in *Solid State Physics under Pressure: Recent Advance with Anvil Devices*, edited by S. Minomura (Springer-Verlag, N.Y., 1985) p. 259.
- ³¹ T. C. Kobayashi, K. Hashimoto, S. Eda, K. Shimizu, K. Amaya, and Y. Onuki, Physica B: Cond. Mat., **281**, 553-554 (2000).
- ³² N. N. Sirota, V. V. Novikov, and A. V. Novikov, Phys. Sol. State **42**, 2093-2096 (2000).
- ³³ See, for example: J. S. Schilling, Adv. Phys. **28**, 657 (1979).
- ³⁴ From Ref³⁰ the value of the resistivity at T_{\min} at ambient pressure is $\sim 78 \mu\Omega\text{cm}$, thus allowing us to calibrate the resistance values in Fig. 2.
- ³⁵ S. Nakamura, T. Goto, S. Kunii, K. Iwashita, and A. Takami, J. Phys. Soc. Jpn. **63**, 623-636 (1994).
- ³⁶ B. Lüthi, S. Blumenröder, B. Hillebrands, E. Zirngiebl, G. Güntherodt, and K. Winzer, Z. Phys. B, **58**, 31-38 (1984).
- ³⁷ T. Gürel and R. Eryiğit, Phys. Rev. B **82**, 104302 (2010).
- ³⁸ Sandeep, M. P. Ghimire, D. P. Rai, P. K. Patra, A. K. Mohanty, and R. K. Thapa, J. Phys.: Conf. Series **377**, 012084 (2012).
- ³⁹ N. R. James, S. Legvold, and F. H. Spedding, Phys. Rev. **88**, 1092 (1952).